RSC Advances

PAPER

View Article Online
View Journal | View Issue

Cite this: *RSC Adv.*, 2019, **9**, 18302

Synthesis and structure of $[(Ph_3P)_2Cu(\mu\text{-}SeCH_2Ph)_2In(SeCH_2Ph)_2]$ as a single-source precursor for the preparation of $CuInSe_2$ nanomaterials†

Manoj K. Pal,[a] Sandip Dey,[a]* Suman Neogy[b] and Mukesh Kumar[c]

Received 7th May 2019
Accepted 27th May 2019

DOI: 10.1039/c9ra03429c

rsc.li/rsc-advances

The reaction of freshly prepared $Na[In(SeCH_2C_6H_5)_4]$ with the mixture of CuCl and triphenylphosphine in methanol yielded $[(PPh_3)_2CuIn(SeCH_2C_6H_5)_4]$. The X-ray structure of the complex revealed the monomeric form of $[(Ph_3P)_2Cu(\mu\text{-}SeCH_2Ph)_2In(SeCH_2Ph)_2]$ consisting of tetrahedral Cu(I) and In(III) centers, bridged by two benzyl selenolate ligands. The complex on pyrolysis in a furnace or in oleylamine/HDA yielded tetragonal $CuInSe_2$. The morphology and composition of nanostructures were investigated by pXRD, SEM, TEM and EDX analysis. The band gap of the $CuInSe_2$ nanostructures, obtained from pyrolysis in HDA and OA has been deduced from DRS as 1.85 and 1.86 eV, respectively.

Introduction

The ternary chalcogenides $CuME_2$ (M = Ga, In; E = S, Se) have been established as the key components in several optoelectronic applications such as photovoltaics (PV), light-emitting diodes and photocatalytic H_2 generations depending on their compositions.[1–4] The direct band gap (1.04–2.50 eV), high absorption coefficients, good radiation stability, non-toxic nature and low cost, make these compounds suitable candidates for the fabrication of next generation PV devices.[2,5–8] In particular, the $CuInSe_2$ (CIS) semiconductor with a band gap of 1.04 eV and absorption coefficient of the order of 10^5 cm^{-1} for photons,[9] is being considered as the nearest competitor to the Si-based PVs in the market.[1,4] However the CIS based PV devices were fabricated employing vacuum- and energy-demanding processes, thus hindering its commercialization.[1,10] In the last decade, solution-based processes, screen printing, spray printing have evolved as alternative technologies for making low-cost solar cells.[8] Moreover, the morphology and size of the pyrolyzed materials can be better controlled by the colloidal synthesis of nanoparticles than by the chemical vapour deposition (CVD) method.[2]

CIS nanoparticles have been prepared by a solution-based one step process using three different sources of Cu, In and Se with capping agents to control the size, shape and morphology of the particles.[1,7,10–12] The various solution-based methods such as solvothermal, electrodeposition and spray pyrolysis used three different sources of precursors to synthesize the CIS materials, which can affect the cell performances depending on the nature of absorbing layer.[10] The solvothermal route under mild reaction conditions using single-source precursors (SSPs) has emerged as highly efficient tool for the controlled preparation of nanostructures. Since the first report of $[(PPh_3)_2CuIn(SEt)_4]$ in 1993 by Hirpo *et al.*,[13] the complexes of the general formula $[(PR_3)_nCuM(ER')_4]$ (R, R′ = alkyl, aryl)[5,13–16] have been extensively investigated as SSPs for the preparation of thin film of $CuME_2$ using CVD technique. A few such SSPs have also been used to prepare the nanoparticles of $CuME_2$ at reduced temperature.[2,3,5] The organic groups R, R′ play significant role in determining the solubility, structure and also the decomposition process of the complex, which affects the phase purity of the semiconductor materials.

We have recently synthesized the complexes of Cu(I) and In(III) metals,[16] using the hybrid ligands amino-alkylselenolates[17,18] and 4-pyridylselenolates[19,20] and prepared the binary copper and indium selenides. The hard donor N atom present in the above ligands, inhibited to form the SSPs containing Cu, In and Se element, either by chelating or bridging with metal centers thus forming co-ordination polymers. However, the ternary $CuInSe_2$ was prepared using two source precursors. To prepare the SSPs for CIS nanomaterials, next we sought to explore the ligand Bz_2Se_2 which is photosensitive[21] and known for clean-cleavage of benzyl group (Bz = CH_2Ph).[22] Herein, we describe the synthesis and structural

[a]*Chemistry Division, Bhabha Atomic Research Centre, India. E-mail: dsandip@barc.gov.in*

[b]*Mechanical Metallurgy Division, Bhabha Atomic Research Centre, India*

[c]*Radiation Biology and Health Sciences Division, Bhabha Atomic Research Centre, Mumbai 400 085, India*

† Electronic supplementary information (ESI) available: Details of crystallographic procedure and structure refinement data table of $[(PPh_3)_2CuIn(SeCH_2C_6H_5)_4]$. ^1H and $^{31}P\{^1H\}$ NMR spectrum and TGA curve of $[(PPh_3)_2CuIn(SeCH_2C_6H_5)_4]$, XRD patterns, SEM images, EDX spectrum and TEM images of $CuInSe_2$. CCDC 1911532. For ESI and crystallographic data in CIF or other electronic format see DOI: 10.1039/c9ra03429c

characterization of $[(PPh_3)_2Cu(\mu\text{-}SeCH_2Ph)_2In(SeCH_2Ph)_2]$, which has been used as SSP for the preparation of single phase $CuInSe_2$ nanoparticles by solvothermal method. The particles were characterized by powder X-ray diffraction (XRD), scanning electron microscopy with energy dispersive X-ray (SEM-EDX) analysis, high-resolution transmission electron microscopy (HRTEM) and diffuse reflectance spectroscopy (DRS).

Results and discussion

Syntheses and NMR spectroscopy

The complex has been synthesized by modifying the procedure reported by Kanatzidis,[13] using mixture of CuCl and PPh_3 instead of $[(Ph_3P)_2Cu(CH_3CN)_2][PF_6]$. The complex $[(PPh_3)_2CuIn(SeCH_2C_6H_5)_4]$ has been synthesized by the addition of CuCl and PPh_3 to a freshly prepared Na-salt of anionic complex of In(III) prepared from $InCl_3$ and four equivalents of Na-salt of benzylselenolate ligand (Scheme 1).[23] This complex has been characterized by elemental analysis and NMR spectroscopy. The microanalysis and integration of the ^1H NMR peaks of the complex suggest the phosphine and selenolate ligands are in 1 : 2 ratio, conforming the formula $[(PPh_3)_2CuIn(SeCH_2C_6H_5)_4]$. The mononuclear structure has been confirmed by the single crystal X-ray structure. The ^1H NMR spectrum exhibits one set of signals for all the selenolato groups in solution. A singlet at δ 3.77 ppm was observed for $SeCH_2$ group in ^1H NMR spectra (Fig. S1, ESI†). The broad singlet was observed at −4.1 ppm in $^{31}P\{^1H\}$ NMR recorded in $CDCl_3$ solvent (Fig. S2, ESI†). The complex is soluble in chloroform, dichloromethane and acetonitrile, but insoluble in methanol.

In contrast to the complexes of Cu and In using ethyl selenolate/phenyl selenolate,[5,13,15] the pyridylselenolates of Cu and In do not react with each other to form heterometallic chalcogenolates.[16] This non reactivity can be attributed to the presence of the pyridine donors, which compete effectively with bridging selenolate ligands for access to the metal coordination sphere to form molecular indium compounds and to the stabilizing influence of the Cu–Cu bonds in the copper compounds.

Crystallography

Molecular structure of $[(PPh_3)_2CuIn(SeCH_2C_6H_5)_4]$ has been established by single crystal X-ray diffraction analyses. The ORTEP drawing with crystallographic numbering scheme is shown in Fig. 1 and the selected inter atomic parameters are given in Table 1. The structure of the complex reveal the monomeric form of $[(Ph_3P)_2Cu(\mu\text{-}SeCH_2Ph)_2In(SeCH_2Ph)_2]$. The tetrahedral Cu(I) and In(III) metals are linked by two bridging benzyl selenolate ligands, forming a planar "$CuSe_2In$" ring. Other two terminal positions of the metal centers are coordinated by two PPh_3 and two benzylselenolate groups. The inner angle Se1–In–Se1^i (98.0°) of the "$CuSe_2In$" ring and outer angle Se2–In–Se2^i (111.1°) formed by the terminal selenolate groups are less deviated from the ideal tetrahedral angle in comparison to the corresponding angles (96.1 and 116.6) in the reported complex $[(Ph_3P)_2Cu(\mu\text{-}SePh)_2In(SePh)_2]$.[15] The spacer CH_2 group of the benzylselenolate ligand in the present complex helps to minimise the steric repulsion between the bulkier groups which is manifested in the reduced non-bonded Cu···In distance of about 3.35 Å, compared to analogous phenyl selenolate complex (3.50 Å).[15] The benzyl groups adopt *anti* conformation and a two-fold symmetry axis exist along the Cu–In bond in the molecular structure. As expected the tetrahedral Cu center is more distorted due to the two bulkier phosphines as revealed by the P1–Cu–P1^i angle measuring 122.2°. The In–Se bond distances (2.62 Å) for the bridging selenolates are longer than the corresponding distances for the terminal selenolates

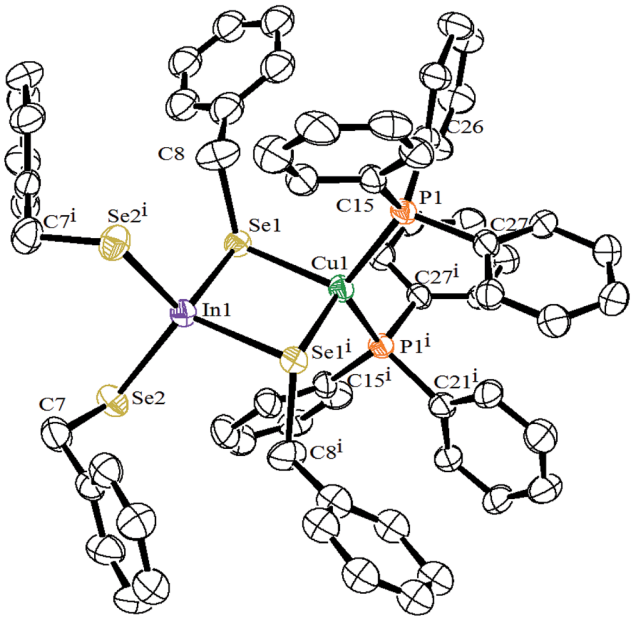

Fig. 1 Molecular structure of $[(PPh_3)_2CuIn(SeCH_2C_6H_5)_4]$.

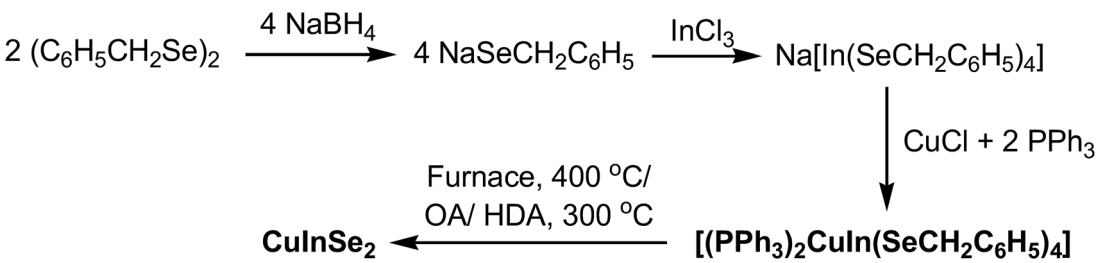

Scheme 1

Table 1 Selected bond lengths (Å) and angles (°) for $[(PPh_3)_2CuIn(SeCH_2C_6H_5)_4]$

In1–Se1	2.6225 (13)	In1–Se2	2.5483 (13)
In1–Se1^i	2.6225 (13)	In1–Se2^i	2.5483 (13)
Cu1–Se1	2.5623 (16)	Cu1–Se1^i	2.5624 (16)
Se1–C8	1.995 (14)	Se2–C7	1.992 (14)
Cu1–P1	2.290 (2)	Cu1–P1^i	2.290 (2)
Cu1⋯In1	3.347		
Se1–In1–Se1^i	98.02 (6)	Se1–In1–Se2	113.36 (4)
Se2–In1–Se2^i	111.11 (7)	Se1–In1–Se2^i	110.21 (4)
Se1–Cu1–Se1^i	101.17 (8)	Cu1–Se1–In1	80.41 (5)
P1–Cu1–Se1	101.92 (7)	P1^i–Cu1–Se1	114.04 (7)
P1–Cu1–Se1^i	114.04 (7)	P1^i–Cu1–Se1^i	101.92 (7)
P1–Cu1–P1^i	122.19 (14)		

(2.55 Å) and are in agreement with earlier reports.[15,16,24,25] The Cu–Se bond distances (2.56 Å) are in the range of reported values.[15,16,24]

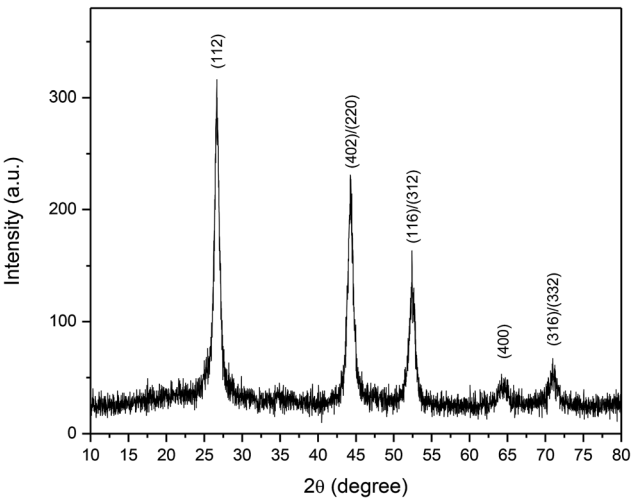

Fig. 2 The PXRD pattern of $CuInSe_2$ obtained from thermolysis of $[(PPh_3)_2CuIn(SeCH_2C_6H_5)_4]$ in oleylamine at 300 °C for 30 min.

Thermal studies

To assess the suitability of the complex as precursor for the preparation of $CuInSe_2$, thermo-gravimetric analysis of $[(PPh_3)_2CuIn(SeCH_2C_6H_5)_4]$ was carried out up to the temperature 800 °C under a flowing argon atmosphere (Fig. S3, ESI†). The complex underwent nearly one step of decomposition with the formation of a black residue. At the end of decomposition at approximately 375 °C, the weight loss found is ~75%, whereas the calculated weight loss is 75.7% for the formation of $CuInSe_2$. The complex $[(PPh_3)_2CuIn(SeCH_2C_6H_5)_4]$ on heating in furnace at 400 °C for 2 h yielded a black residue (weight loss found 74.4%; calcd 75.7%), which was characterized as tetragonal $CuInSe_2$ by powder XRD (Fig. S4, ESI†) (JCPDS file no. 75-0107). The XRD pattern of the residue obtained on furnace heating showed additional small intense peaks attributed to the planes (200) and (211).[13,26] These peaks are absent in the XRD pattern of residues obtained from solvolysis of the precursor either in OA or HDA attributing to the nano-crystalline nature of residues. The energy dispersive X-ray analysis (EDX) of the black powder obtained on furnace heating showed the presence of Cu, In and Se atoms (Table 2) (Fig. S5, ESI†). The scanning electron micrographs (SEM) taken at different resolutions (Fig. S6, ESI†), showed large aggregates of $CuInSe_2$ micro-crystals.

Thermolysis of $[(PPh_3)_2CuIn(SeCH_2C_6H_5)_4]$ in OA at 300 °C for 30 min, resulted a black powder of $CuInSe_2$ of body centered tetragonal phase, confirmed by powder XRD (Fig. 2) (JCPDS file no. 81-1936). The broadening of the peaks suggests the formation of nanoparticles with the average size of ~15 nm, calculated using the Debye–Scherrer formula. The EDX of the black powder showed the presence of Cu, In and Se atoms (Table 2 and Fig. S7, ESI†). The SEM taken at different resolutions (Fig. S8, ESI†), showed large aggregates of $CuInSe_2$ nanocrystals. The TEM image of the $CuInSe_2$ nanoparticles showed irregular shapes with size in the range of 10–25 nm (Fig. 3(a)). The high-resolution TEM (HRTEM) image of $CuInSe_2$ nanoparticle is displayed in Fig. 3(b). The observed inter-planar spacing of 0.34 nm is complied with the (112) lattice spacing of $CuInSe_2$ nanoparticles. The ring-type selected area electron diffraction (SAED) pattern (Fig. 3(c)) from the particles corroborated their nanocrystalline nature.

Thermolysis of $[(PPh_3)_2CuIn(SeCH_2C_6H_5)_4]$ in HDA at 300 °C for 30 min, resulted in a black powder, the XRD confirmed body centered tetragonal phase of $CuInSe_2$ (Fig. S9, ESI†) (JCPDS file no. 81-1936). The broadening of the peaks suggests the formation of nanoparticles with an average size of ~15 nm calculated using the Debye–Scherrer formula. The EDX of the black powder showed the presence of Cu, In and Se atoms (Table 2) (Fig. S10, ESI†). The scanning electron micrographs (SEM) taken at different resolutions (Fig. S11, ESI†), showed large aggregates of nano-crystalline

Table 2 The energy dispersive X-ray analysis (EDX) of the $CuInSe_2$ obtained on thermal decomposition of $[(PPh_3)_2CuIn(SeCH_2C_6H_5)_4]$

	Atomic ratio	Atomic weight percentage found (calcd)		
Experiment	Cu : In : Se	Cu	In	Se
Furnace heating at 400 °C for 2 h	28.05 : 25.50 : 46.45 (1.10 : 1 : 1.82)	21.27 (18.90)	34.94 (34.14)	43.78 (46.96)
Solvolysis in OA at 300 °C for 30 min	25.61 : 24.79 : 49.60 (1.03 : 1 : 2)	19.39 (18.90)	33.93 (34.14)	46.68 (46.96)
Solvolysis in OA at 300 °C for 10 min	20.38 : 27.41 : 52.21 (1 : 1.34 : 2.56)	15.12 (18.90)	36.75 (34.14)	48.13 (46.96)
Solvolysis in HDA at 300 °C for 30 min	25.29 : 25.93 : 48.78 (1 : 1.03 : 1.93)	19.05 (18.90)	35.29 (34.14)	45.66 (46.96)

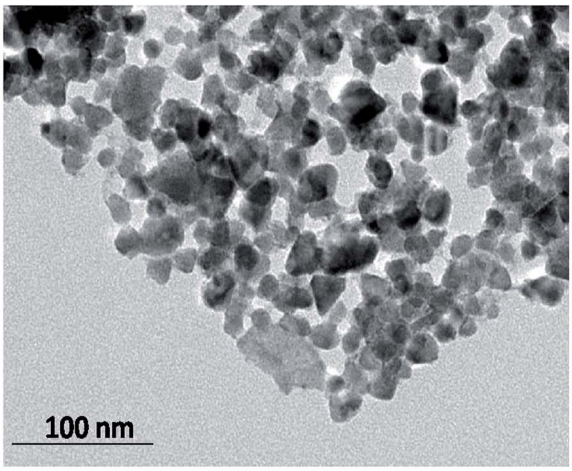

(a)

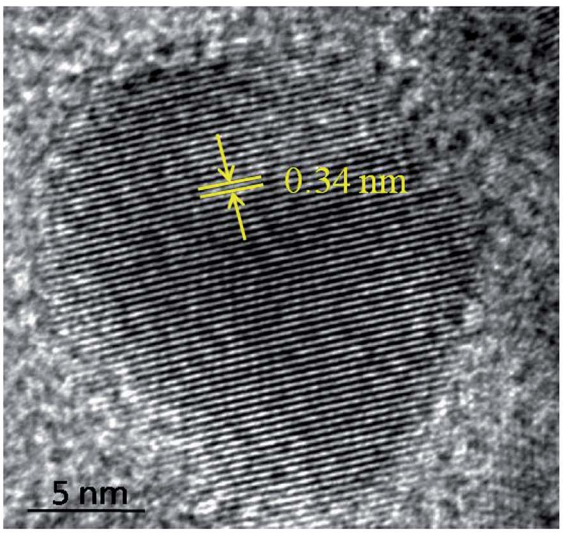

(b)

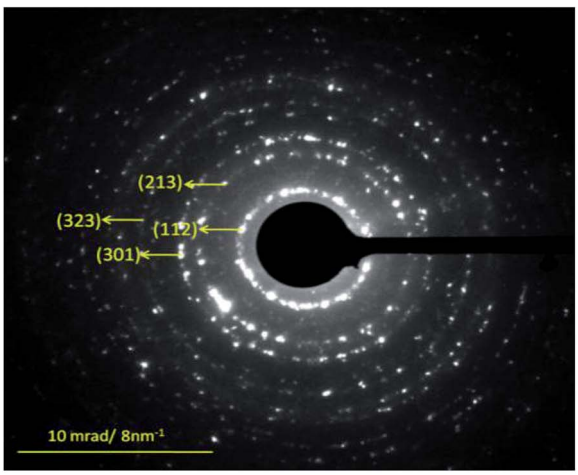

(c)

Fig. 3 (a) TEM image, (b) HRTEM image, and (c) SAED pattern of the $CuInSe_2$ nanoparticles obtained from thermolysis of $[(PPh_3)_2CuIn(SeCH_2C_6H_5)_4]$ in oleylamine at 300 °C for 30 min.

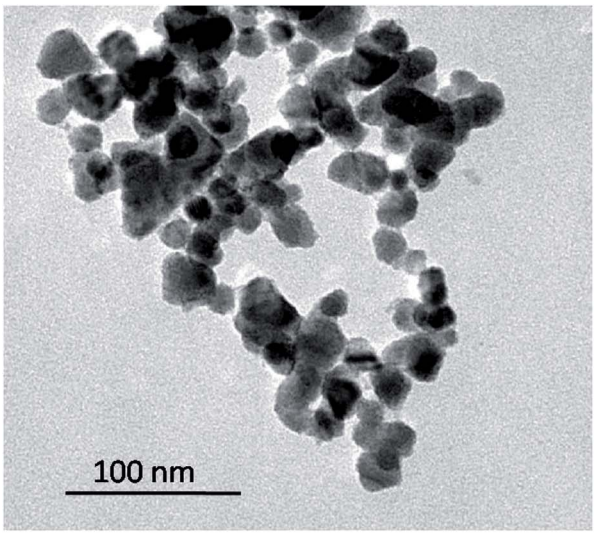

(a)

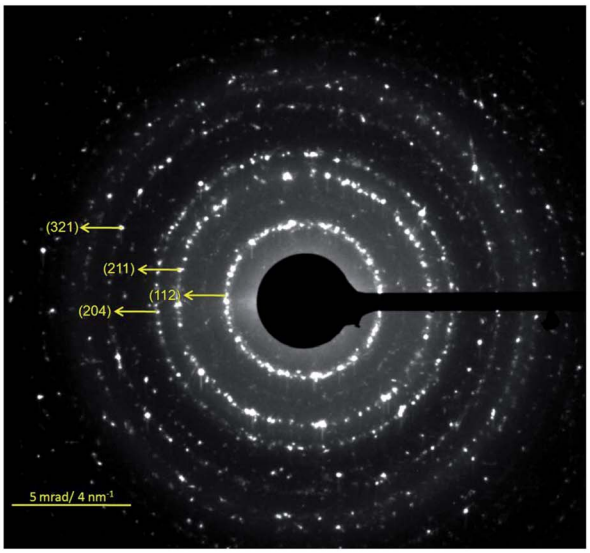

(b)

Fig. 4 (a) TEM image, (b) SAED pattern of the $CuInSe_2$ nanoparticles obtained from thermolysis of $[(PPh_3)_2CuIn(SeCH_2C_6H_5)_4]$ in hexadecylamine at 300 °C for 30 min.

$CuInSe_2$. The TEM image of the resultant $CuInSe_2$ nanoparticles (Fig. 4(a)) show irregular shapes with size in the range of 20–30 nm. The ring-type SAED pattern (Fig. 4(b)) from the particles corroborated their nanocrystalline nature.

The complex $[(PPh_3)_2CuIn(SeCH_2C_6H_5)_4]$ on thermolysis in oleylamine at 300 °C for 10, 20 and 30 min time interval also gave the tetragonal $CuInSe_2$ as indicated by powder XRD (Fig. S12, ESI†). The powder XRD pattern obtained for 10, 20 and 30 min are almost similar in appearance and the size of the particles calculated using the Debye–Scherrer formula are ~20 nm. The EDX of the black powder obtained in OA at 300 °C for 10 min showed the presence of Cu, In and Se atoms (Table 2) (Fig. S13, ESI†). The SEM taken at different resolutions (Fig. S14, ESI†), showed large aggregates of nano-crystalline $CuInSe_2$.

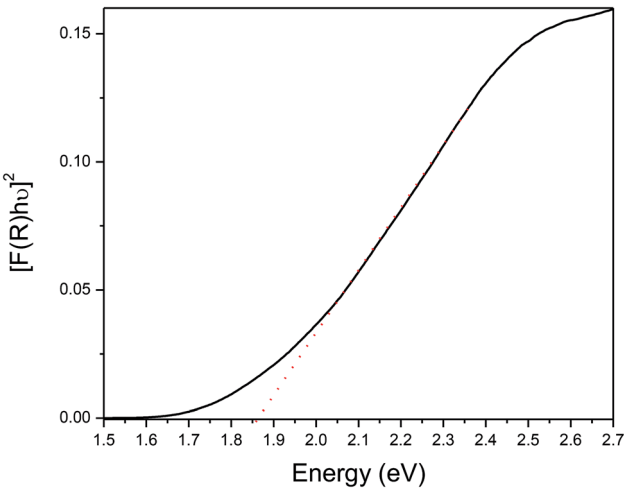

Fig. 5 Plots of $[F(R)h\nu]^2$ *vs.* energy generated by Kubelka–Munk transformation of solid-state diffuse reflectance data $CuInSe_2$ nanostructures obtained by thermolysis of $[(PPh_3)_2CuIn(SeCH_2C_6H_5)_4]$ in OA at 300 °C for a duration of 30 minutes.

Optical properties of $CuInSe_2$ nanostructures

The optical band gap of $CuInSe_2$ nanostructures has been measured by solid state diffuse reflectance spectroscopy (DRS) applying Kubelka–Munk transformations. The plot of $[F(R)h\nu]^2$ *vs.* $h\nu$, has provided the direct band gap value 1.86 eV for $CuInSe_2$, obtained on thermolysis of $[(PPh_3)_2CuIn(SeCH_2C_6H_5)_4]$ in oleylamine at 300 °C (Fig. 5). Similarly, the direct band gap has been calculated as 1.85 eV for $CuInSe_2$ obtained on thermolysis of $[(PPh_3)_2CuIn(SeCH_2C_6H_5)_4]$ in hexadecylamine at 300 °C (Fig. S15, ESI†) and matches well with the reported values.[27] The direct band gaps of $CuInSe_2$ nanostructures showed a blue shift compared to the bulk $CuInSe_2$ *i.e.* 1.04 eV.[28] The increase in band gap with decreasing particle size may be either due to lattice distortions or surface lattice defect or quantum confinement or surface effect of the carriers.[29]

Conclusions

The stable hetero-bimetallic complex of copper and indium metals of benzylselenolate ligand is conveniently synthesized, which can be used as SSP for the preparation of $CuInSe_2$. The mononuclear structure of the complex reveals the monodentate and bridging mode of selenolate ligands. On thermolysis in oleylamine or HDA, the complex yielded pure-phase of $CuInSe_2$ nanocrystals, which showed the band gap of 1.86 and 1.85 eV, respectively. The morphology and composition of nanostructures have been investigated by pXRD, SEM, TEM and EDX analysis.

Experimental section

Materials and methods

All the reactions were carried out in Schlenk flasks under a nitrogen/argon atmosphere. Indium trichloride, CuCl, PPh_3, $NaBH_4$, oleylamine (OA), hexadecylamine (HDA) and analytical grade solvents were obtained from commercial sources. The ligand $(C_6H_5CH_2Se)_2$ was prepared according to literature method.[30] Due to slow photo-decomposition of Bz_2Se_2, it was recrystallized every month from hexane. Melting points were determined in capillary tubes and are uncorrected. Elemental analyses were carried out on a Thermo Fischer Flash EA1112 CHNS elemental analyzer. The ^1H and $^{31}P\{^1H\}$ NMR spectra were recorded on a Varian spectrometer operating at 500 and 242.9 MHz, respectively. Chemical shifts are relative to internal chloroform peak for ^1H NMR spectra. Thermo gravimetric analyses (TGA) were carried out on a Nitzsch STA 409 PC-Luxx TG-DTA instrument, which was calibrated with $CaC_2O_4 \cdot H_2O$. The TG curves were recorded at a heating rate of 10 °C min^{-1} under a flow of argon. Powder diffraction X-ray pattern were obtained on a Rigaku SmartLab X-ray diffractometer using CuKα radiation. SEM and EDX measurements were carried out on MIRERO Inc. AIS2100 and Oxford INCA E350 instruments, respectively. The TEM investigations were carried out in a Libra 200FE instrument operated at 200 kV. Optical diffuse reflectance measurements in the region 200–1800 nm (0.68 eV to 6.2 eV) were conducted on a two-beam spectrometer (V-670, JASCO) with a diffuse reflectance (DR) attachment consisting of an integration sphere coated with barium sulfate which was used as a reference. Measured reflectance data were converted to absorption (A) using Kubelka–Munk remission function.[31]

Syntheses

$[(PPh_3)_2CuIn(SeCH_2C_6H_5)_4]$. To a freshly prepared $NaSeCH_2C_6H_5$ (from $(C_6H_5CH_2Se)_2$ (142 mg, 0.42 mmol) and $NaBH_4$ (33 mg, 0.87 mmol) in benzene/methanol (20 mL)) was added solid $InCl_3$ (46 mg, 0.21 mmol) and stirred for 1 h. To this, CuCl (21 mg, 0.21 mmol) and PPh_3 (110 mg, 0.42 mmol) dissolved in dichloromethane/CH_3CN (20 mL) was added, the stirring was continued for 4 h. The reaction mixture was filtered through G3 assembly, the off-white residue was washed with H_2O, methanol (2 × 5 mL), and dried in vacuum to give the title complex (yield 176 mg, 61%), mp 161 °C. Anal. calcd for $C_{64}H_{58}CuInP_2Se_4$: C, 55.57; H, 4.23%. Found: C, 55.16; H, 4.19%. ^1H NMR ($CDCl_3$): δ 3.77 (s, 8H, $SeCH_2$); 7.12 (t, $^3J_{HH} = 7.0$ Hz, 12H, Ph); 7.16 (q, $^3J_{HH} = 6.5$ Hz, 8H, Ph); 7.22–7.25 (m, 24H, PPh); 7.34 (t, $^3J_{HH} = 6.5$ Hz, 8H, Ph) ppm. $^{31}P\{^1H\}$ NMR ($CDCl_3$): δ − 4.1 (br, s) ppm.

Preparation of $CuInSe_2$ by solvothermal method

The complex $[(PPh_3)_2CuIn(SeCH_2C_6H_5)_4]$ (95 mg) was added in oleylamine/HDA (~5 mL) preheated at 300 °C with vigorous stirring under flowing argon and continued for 30 minutes. The reaction temperature was rapidly brought down to 60 °C and was quenched by injecting 10 mL of methanol. The resulting residue, thus obtained was separated by washing with excess methanol followed by centrifuging and drying under vacuum to obtain black powder.

Conflicts of interest

There are no conflicts of interest to declare.

Acknowledgements

We thank Mr Asheesh Kumar of Chemistry Division for the measurement of SEM and EDX.

References

1 V. Sousa, B. F. Gonçalves, M. Franco, Y. Ziouani, N. González-Ballesteros, M. Fátima Cerqueira, V. Yannello, K. Kovnir, O. I. Lebedev and Y. V. Kolen'ko, *Chem. Mater.*, 2019, **31**, 260–267.
2 S. L. Castro, S. G. Bailey, R. P. Raffaelle, K. K. Banger and A. F. Hepp, *Chem. Mater.*, 2003, **15**, 3142–3147.
3 J. J. Nairn, P. J. Shapiro, B. Twamley, T. Pounds, R. von Wandruszka, T. R. Fletcher, M. Williams, C. Wang and M. G. Norton, *Nano Lett.*, 2006, **6**, 1218–1223.
4 H. Takahashi, H. Fujiki, S. Yokoyama, T. Kai and K. Tohji, *Nanomaterials*, 2018, **8**, 221–234.
5 K. K. Banger, M. H.-C. Jin, J. D. Harris, P. E. Fanwick and A. F. Hepp, *Inorg. Chem.*, 2003, **42**, 7713–7715.
6 O. Kluge, R. Biedermann, J. Holldorf and H. Krautscheid, *Chem.–Eur. J.*, 2014, **20**, 1318–1331.
7 C.-C. Wu, C.-Y. Shiau, D. W. Ayele, W.-N. Su, M.-Y. Cheng, C.-Y. Chiu and B.-J. Hwang, *Chem. Mater.*, 2010, **22**, 4185–4190.
8 S. N. Malik, S. Mahboob, N. Haider, M. A. Malik and P. O'Brien, *Nanoscale*, 2011, **3**, 5132–5139.
9 A. Rockett and R. W. Birkmire, *J. Appl. Phys.*, 1991, **70**, R81–R97.
10 J. Lee, S.-H. Lee, J.-S. Hahn, H.-J. Sun, G. Park and J. Shim, *J. Nanosci. Nanotechnol.*, 2014, **14**, 9313–9318.
11 D. S. I. Jebakumar, B. Chitara and S. B. Krupanidhi, *J. Nanosci. Nanotechnol.*, 2017, **17**, 1538–1542.
12 M. A. Malik, P. O'Brien and N. Revaprasadu, *Adv. Mater.*, 1999, **11**, 1441–1444.
13 W. Hirpo, S. Dhingra, A. C. Sutorik and M. G. Kanatzidis, *J. Am. Chem. Soc.*, 1993, **115**, 1597–1599.
14 K. K. Banger, J. Cowen and A. F. Hepp, *Chem. Mater.*, 2001, **13**, 3827–3829.
15 J. Masnovi, K. K. Banger, P. E. Fanwick and A. F. Hepp, *Polyhedron*, 2015, **102**, 246–252.
16 M. K. Pal, S. Dey, A. P. Wadawale, N. Kushwah, M. Kumar and V. K. Jain, *ChemistrySelect*, 2018, **3**, 8575–8580.
17 S. Dey, V. K. Jain, S. Chaudhury, A. Knoedler, F. Lissner and W. Kaim, *J. Chem. Soc., Dalton Trans.*, 2001, 723–728.
18 G. Kedarnath, S. Dey, V. K. Jain and G. K. Dey, *J. Nanosci. Nanotechnol.*, 2006, **6**, 1031–1037.
19 K. V. Vivekananda, S. Dey, A. Wadawale, N. Bhuvanesh and V. K. Jain, *Dalton Trans.*, 2013, **42**, 14158–14167.
20 G. K. Kole, K. V. Vivekananda, M. Kumar, R. Ganguly, S. Dey and V. K. Jain, *CrystEngComm*, 2015, **17**, 4367–4376.
21 J. Y. C. Chu, D. G. Marsh and W. H. H. Guenther, *J. Am. Chem. Soc.*, 1975, **97**, 4905–4908.
22 S. Dey, V. K. Jain and B. Varghese, *J. Organomet. Chem.*, 2001, **623**, 48–55.
23 M. T. Ng and J. J. Vittal, *Inorg. Chem.*, 2006, **45**, 10147–10154.
24 Y.-G. Han, C. Xu, T. Duan and Q.-F. Zhang, *Inorg. Chim. Acta*, 2011, **365**, 414–418.
25 K. Holligan, P. Rogler, D. Rehe, M. Pamula, A. Y. Kornienko, T. J. Emge, K. Krogh-Jespersen and J. G. Brennan, *Inorg. Chem.*, 2015, **54**, 8896–8904.
26 J. Zhang, W. Que, F. Shen and Y. Liao, *Sol. Energy Mater. Sol. Cells*, 2012, **103**, 30–34.
27 G. Karmakar, A. Tyagi, A. Wadawale, G. Kedarnath, A. P. Srivastava, C. A. Betty and V. Singh, *ChemistrySelect*, 2018, **3**, 10394–10401.
28 S. Chichibu, T. Mizutani, K. Murakami, T. Shioda, T. Kurafuji, H. Nakanishi, S. Niki, P. J. Fons and A. Yamada, *J. Appl. Phys.*, 1998, **83**, 3678–3689.
29 M. X. Wang, G. H. Yue, Y. D. Lin, X. Wen, D. L. Peng and Z. R. Geng, *Nano-Micro Lett.*, 2013, **5**, 1–6.
30 J. Q. Li, W. L. Bao, P. Lue and X. J. Zhou, *Synth. Commun.*, 1991, **21**, 799–806.
31 B. Philips-Invernizzi, D. Dupont and C. Cazé, *Opt. Eng.*, 2001, **40**, 1082–1092.